The Relationship Between Blue-Fundus Autofluorescence and Optical Coherence Tomography in Eyes With Lamellar Macular Holes

Roberto dell'Omo,[1] Denise Vogt,[2] Ricarda G. Schumann,[2] Serena De Turris,[1] Gianni Virgili,[3] Giovanni Staurenghi,[4] Matteo Cereda,[4] Ciro Costagliola,[1] Siegfried G. Priglinger,[2] and Ferdinando Bottoni[4]

[1]Department of Medicine and Health Sciences "Vincenzo Tiberio," University of Molise, Campobasso, Italy
[2]Department of Ophthalmology, Ludwig-Maximilians-University, Munich, Germany
[3]Department of Translational Surgery and Medicine, University of Florence, Florence, Italy
[4]Department of Biomedical and Clinical Science "Luigi Sacco," Sacco Hospital, University of Milan, Milan, Italy

Correspondence: Roberto dell'Omo, Department of Medicine and Health Sciences "Vincenzo Tiberio," University of Molise, Via Francesco De Sanctis 1, 86100 Campobasso, Italy; roberto.dellomo@unimol.it.

Submitted: March 18, 2018
Accepted: May 18, 2018

Citation: dell'Omo R, Vogt D, Schumann RG, et al. The relationship between blue-fundus autofluorescence and optical coherence tomography in eyes with lamellar macular holes. *Invest Ophthalmol Vis Sci*. 2018;59:3079–3087. https://doi.org/10.1167/iovs.18-24379

Purpose. The purpose of this study was to evaluate the relationship between blue-fundus autofluorescence (B-FAF) and optical coherence tomography (OCT) in eyes with lamellar macular holes (LMHs).

Methods. this was a multicenter, observational case series. Ninety-two eyes with LMH associated with the standard epiretinal membrane (ERM) or lamellar hole–associated epiretinal proliferation (LHEP) were evaluated. The eyes must also present an area of increased autofluorescence on B-FAF.

Results. The ERM-alone group and the LHEP group differed with respect to the following variables: logarithm of the minimum angle of resolution best-corrected visual acuity (0.13 ± 0.13 vs. 0.25 ± 0.17; $P < 0.001$), central foveal thickness (218.74 ± 52.4 µm vs. 187.28 ± 50.29 µm; $P = 0.008$), FAF diameter (400.78 ± 189.36 µm vs. 503.37 ± 214.25 µm; $P = 0.014$), outer plexiform layer (OPL) diameter (382.10 ± 157.34 µm vs. 550.79 ± 228.05 µm; $P = 0.0001$), and disruption of external limiting membrane and ellipsoid zone, which was noted in only 1 and 3 eyes with ERM alone, respectively, and in 18 and 23 eyes with LHEP, respectively ($P < 0.0001$ for both observations). No difference was found for diameters measured at the level of the inner limiting membrane and schisis/cavitation. In both the ERM-alone group and the LHEP group, a strong correlation was found between the diameters measured on B-FAF and diameters measured at the OPL level on OCT images ($P < 0.0001$ for both groups).

Conclusions. In eyes with LMHs, a strong correlation exists between the diameters of the holes measured with B-FAF and those measured at the OPL level with OCT. This may indicate that the loss or displacement of retinal cells containing macular pigment at the OPL level, specifically photoreceptors and/or Müller cells, is involved in this vitreomaculopathy.

Keywords: lamellar macular hole, optical coherence tomography, fundus autofluorescence, lamellar hole-associated epiretinal proliferation, epiretinal membrane

Short-wavelength (488 nm) blue-fundus autofluorescence (B-FAF) has recently become a standard technique in clinical and research settings to investigate and monitor retinal diseases. The short-wavelength FAF signal is mainly derived from the bisretinoids of lipofuscin in RPE cells, and it depends on variables including the presence and amount of absorptive pigments and structures.[1–3] Macular pigment (MP; absorption maximum: 460 nm) strongly absorbs blue light; thus, a typical eye applies central foveal masking to B-FAF images due to the central accumulation of MP.[4] Any changes to the amount or composition of fluorophores in RPE cells or from its anterior tissues may generate abnormal B-FAF signals.[5]

In full-thickness macular holes (FTMHs), the lack of neurosensory retina at the fovea results in an intense B-FAF signal at the site of the hole.[6] Lamellar macular holes (LMHs) are non-FT macular lesions characterized by an irregular foveal contour, intraretinal splitting or cavitation, and intact or disrupted outer retinal layers. Currently, two main types of LMHs have been identified, based on the appearance of the epiretinal tissue associated with the LMH (either standard epiretinal membrane [ERM] or lamellar hole-associated epiretinal proliferation [LHEP])[7] and other features observed on spectral domain–optical coherence tomography (SD-OCT).[8]

Similar to FTMHs, these two types of LMHs show increased FAF signals relative to the surrounding background,[9] but in contrast to FTMH, the retinal tissue defect in LMH is partial thickness; thus, it is not clear which missing layer causes the increased autofluorescent signal. Because the area of increased autofluorescence might represent the actual loss of foveal tissue or a mere centrifugal displacement of neurosensory tissue containing MP,[10–12] it would be interesting to investigate

the relationship between B-FAF and OCT findings in the eyes with LMH.

The purpose of this study was to compare measurements taken with B-FAF to those taken with OCT at different levels of the LMHs associated with standard ERM and/or LHEP.

Methods

This was an observational three-center study in which patients with LMH were examined with B-FAF and SDOCT according to prespecified imaging protocols.

Patients were seen at the Department of Medicine and Health Sciences, University of Molise, Campobasso, Italy; the Eye Clinic, Department of Clinical Science "Luigi Sacco," Sacco Hospital, University of Milan, Milan, Italy; and the Department of Ophthalmology, Ludwig-Maximilians-University, Munich, Germany, between May and September 2017. The institutional review boards approved the review of the patients' data. The study was conducted according to the tenets of the Declaration of Helsinki. Informed consent was obtained from all participants.

The OCT criteria used to diagnose LMHs were as follows: (1) an irregular foveal contour or a defect in the inner fovea; (2) lamellar separation of the neurosensory retina ("cavitated" or "schitic" in appearance)[8] in at least one horizontal, vertical, or oblique scan; and (3) the absence of a full-thickness foveal defect.

The presence of a standard ERM was determined by a thin and highly reflective line, whereas LHEP was defined by the presence of a material with homogenous, medium reflectivity measuring at least 20 μm, and located on the epiretinal surface.[7]

To be included in the study, the eyes must also present an area of increased autofluorescent signal that colocalized with the inner defect observed in the fovea and was not attributable to an intraretinal cyst, pseudovitelliform deposit, or localized neurosensory detachment at the fovea based on OCT images (Fig. 1). Exclusion criteria included the following: macular disorders (e.g., AMD, macular edema, diabetic retinopathy, retinal vessel occlusion, uveitis); a history of intraocular surgery (except uncomplicated phacoemulsification) or ocular trauma; and myopic refractive error (spherical equivalent) ≥ -6.0 diopters (D) or axial length ≥ 26.5 mm calculated by using partial optical coherence inferometry (IOLMaster; Carl Zeiss Meditec, Inc., Jena, Germany).

Patient characteristics, including age, sex, lens status, refractive error, and the logarithm of the minimum angle of resolution (logMAR) best-corrected visual acuity (BCVA) were recorded.

Imaging Recording and Analysis

All images were collected using the Heidelberg Spectralis system (Heidelberg Engineering, Heidelberg, Germany), which combines an SD-OCT with a confocal scanning laser ophthalmoscope.

B-FAF (excitation wavelength at 488 nm and barrier filter at 500 nm) images and OCT images were obtained after pupil dilation.

The OCT recording protocol consisted of a sequence of 37 horizontal section, spaced 120 μm apart, covering an area of 20 or 30 degrees horizontally by 15 degrees vertically, and a sequence of 24 radial sections recorded in the high-resolution (HR) mode simultaneously with infrared (IR) images.

In addition, simultaneous B-FAF/OCT images were acquired (two perpendicular, horizontal, and vertical OCT sections, centered on the fovea and recorded in HR mode).

Multiple OCT morphologic characteristics were analyzed, including the type of epiretinal material associated with the LMH, the integrity/disruption of the external limiting membrane (ELM), ellipsoid zone (EZ), and the central and minimal foveal thickness (CFT and mFT respectively); the latter was defined as the thinnest part of the fovea corresponding or not to the center of the foveal pit.

The IR/OCT sections enabled detailed detection of the epiretinal material associated with the holes (standard ERM or LHEP or both), but measurements of the holes' diameters were obtained exclusively from one of the two simultaneously recorded B-FAF/OCT images; the higher-quality scan was chosen for analysis (Fig. 2).

Using OCT images, the hole diameters were measured at the inner limiting membrane (ILM) level and intraretinally, at the central borders of the outer plexiform layer (OPL) and at the level of the external borders of the schisis/cavitation, respectively (Fig. 2).

All measurements were performed using the Spectralis built-in manual caliper function on high magnification after adjusting the scale to 1:1 μm, except for CFT, which was calculated using the automated "thickness map" function of the Heidelberg Eye Explorer.

All measurements were taken by two blinded, independent graders (FB and RdO). In the case of a disagreement, a third grader (GS) provided the deciding judgment.

Statistical Analysis

The *t*-test and a χ^2 test were used to compare continuous variables and dichotomous variables, respectively.

Pearson's and Spearman's ρ correlation coefficients were used to test the correlation between diameters of the holes measured on B-FAF and OCT images. Spearman's ρ correlation coefficient was also used to test the correlation between EZ disruption length (determined using OCT) and the diameter of the hole determined using B-FAF. Linear fit plots and linear regression were used to explore the association between the variables. The interrater agreement between graders was determined with weighted κ statistics and intraclass correlation coefficients (ICCs).

$P < 0.05$ was considered statistically significant. All analyses were conducted using the Stata 14.1 software (StataCorp 2015, College Station, TX, USA).

Results

A total of 92 eyes from 92 patients who met the inclusion criteria were enrolled in the study. The mean age (±SD) was 70.5 ± 9.0 years. Of the 92 patients, 35 (38%) were male and 57 (62%) were female; 65 (70.7%) eyes were phakic and 27 (29.3%) eyes were pseudophakic. The refraction (spherical equivalent) of the included eyes ranged between +1.50 and −5.00 D (mean = −1.75 D), and the axial length ranged between 22.5 and 26.1 mm (mean = 23.8 mm).

An analysis of OCT images revealed LHEP in 45 eyes (48.9%). Among these 45, only 5 eyes (5.4%) presented with isolated LHEP, whereas the remaining 40 (43.5%) showed both LHEP and standard ERM. Standard ERM alone was found in 47 eyes (51.1%).

All of the eyes in this series presented with either LHEP or standard ERM.

The group with ERM alone and the group with LHEP (alone or in combination with ERM) differed with respect to the following variables: logMAR BCVA (0.13 ± 0.13 vs. 0.25 ± 0.17, $P < 0.001$), CFT (218.74 ± 52.4 μm vs. 187.28 ± 50.29 μm, $P = 0.008$), mFT (201.11 ± 45.64 μm vs. 156.78 ± 41.26

Investigative Ophthalmology & Visual Science

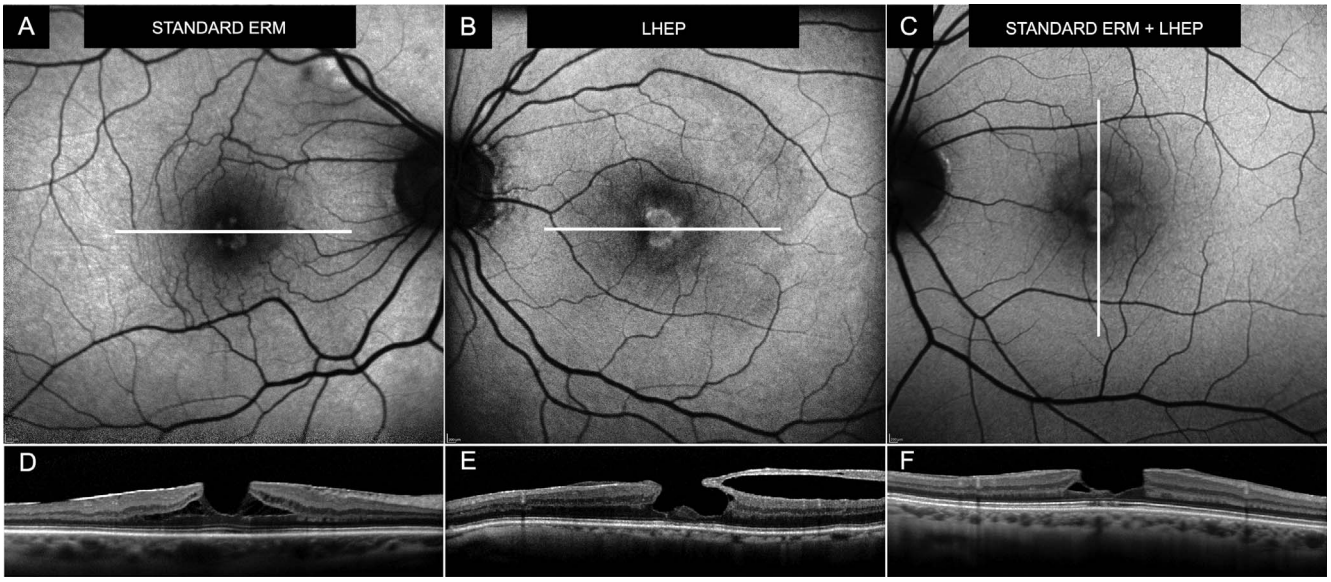

Figure 1. B-FAF (**A**–**C**) and corresponding OCT (**D**–**F**) scans of lamellar macular holes with standard ERMs (**A**, **D**), LHEP (**B**, **E**), and concomitant ERM and LHEP (**C**, **F**). *White line* on B-FAF images indicates the OCT scan level.

μm, $P < 0.0001$), FAF diameter (400.78 ± 189.36 μm vs. 503.37 ± 214.25 μm, $P = 0.014$), OPL diameter (382.10 ± 157.34 μm vs. 550.79 ± 228.05 μm, $P = 0.0001$), and disruption of ELM and EZ, which was noted in only 1 and 3 eyes with ERM alone, respectively, and in 18 and 23 eyes with LHEP, respectively ($P \leq 0.0001$ for both observations). The two groups did not differ with respect to the diameters measured at the level of the ILM (448.01 ± 197.77 μm vs. 520.05 ± 183.86 μm, $P = 0.075$) or at the level of the schisis/cavitation (1257.61 ± 678.17 μm vs. 1127.25 ± 495.28 μm, $P = 0.37$, respectively in the ERM-alone group and the LHEP group). The Table summarizes the B-FAF and OCT findings.

Correlation Between B-FAF and OCT Diameters

Using Pearson's correlation and bootstrap resampling to compare relationships between variables, it was found that overall B-FAF diameter was more strongly correlated with OPL diameter ($r = 0.79$, $P < 0.0001$) than with ILM diameter ($r = 0.59$, $P = 0.007$; Figs. 3–5). The correlations between B-FAF and OPL diameters in the ERM-alone group and the LHEP group were as follows: $r = 0.89$, $P < 0.0001$, 95% confidence interval (CI): 0.81 to 0.94 and $r = 0.75$, $P < 0.0001$, 95% CI: 0.58 to 0.86, respectively.

The correlations between B-FAF and ILM diameters in the ERM-alone group and the LHEP group were as follows: $r = 0.67$, $P < 0.0001$, 95% CI: 0.47 to 0.80 and $r = 0.35$, $P = 0.02$, and 95% CI: 0.048 to 0.59, respectively.

Regression analysis showed that the B-FAF diameter was associated with the ILM diameter, without significant interaction with LHEP. Thus, a regression model was fitted in which ILM diameter and LHEP had no interaction. In this model, B-FAF diameter increased by 54 μm per 100-μm ILM diameter

Table. General Characteristics and BCVA, B-FAF, and OCT Findings of the Sample

	Standard ERM Alone ($n = 47$)	LHEP ($n = 45$)	*P*
Age (y)	68.9 ± 8.7	72.1 ± 9.2	0.089*
Sex			0.21†
Male	15 (31.9%)	20 (44.4%)	
Female	32 (68.1%)	25 (55.6%)	
Lens status			**0.008**†
phakic	39 (83%)	26 (57.8%)	
IOL	8 (17%)	19 (42.2%)	
logMAR BCVA	0.13 ± 0.13	0.25 ± 0.17	**<0.001***
CFT (μm)	218.74 ± 52.4	187.28 ± 50.29	**0.008***
mFT (μm)	201.11 ± 45.64	156.78 ± 41.26	**<0.0001***
B-FAF diameter (μm)	400.78 ± 189.36	503.37 ± 214.25	**0.014***
ILM diameter (μm)	448.01 ± 197.77	520.05 ± 183.86	0.075*
OPL diameter (μm)	382.10 ± 157.34	550.79 ± 228.05	**0.0001***
Schisis/cavitation diameter (μm)	1257.61 ± 678.17	1127.25 ± 495.28	0.37*
Disrupted ELM	1/47 (2.1%)	18/45 (40%)	**<0.0001***
Disrupted EZ	3/47 (6.4%)	23/45 (51.1%)	**<0.0001***

P values in bold are statistically significant. IOL, intraocular lens.
* *t*-test *P* value.
† χ^2 test *P* value.

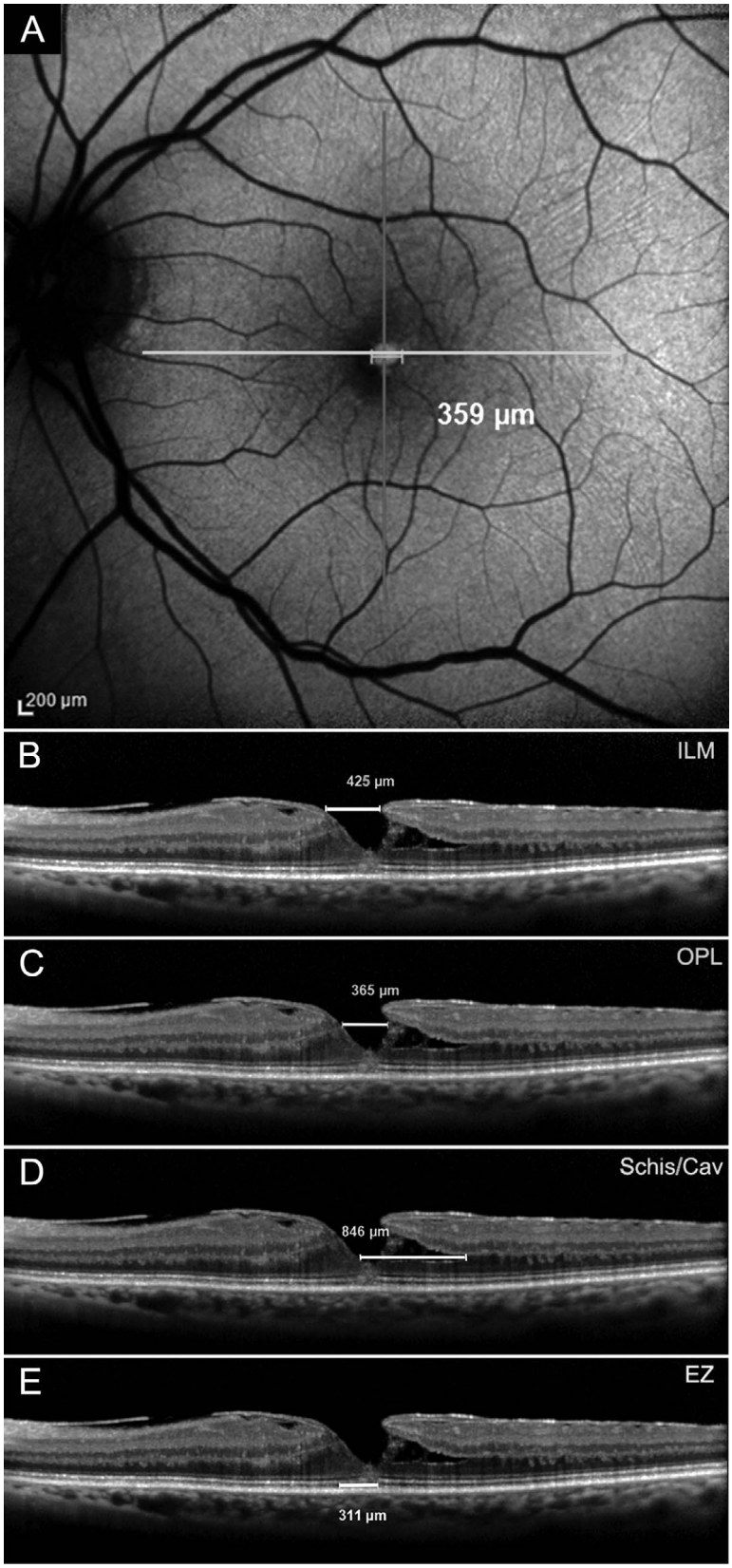

Figure 2. B-FAF (**A**) and OCT-based measurements of the diameter of the hole taken at the ILM level (**B**), OPL (**C**), and schisis/cavitation (Schis/Cav) level (**D**). Measurement of the length of the disrupted EZ is shown in **E**. Measurements were taken manually using the built-in Spectralis software. The *horizontal white arrow* on B-FAF image (**A**) indicates the location of the corresponding OCT scans; the caliper indicates where the horizontal diameter of the hole was measured on B-FAF image.

Investigative Ophthalmology & Visual Science

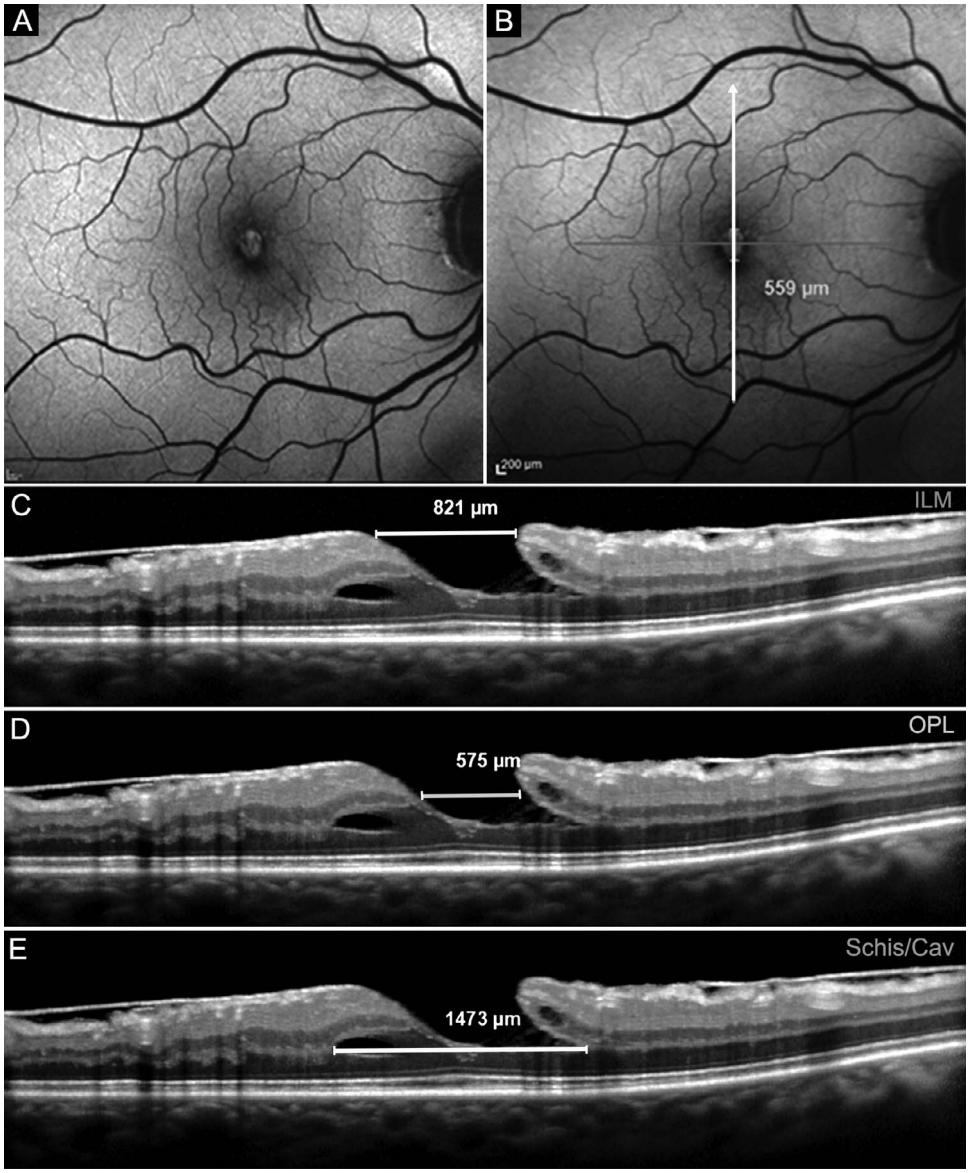

FIGURE 3. B-FAF (**A**, **B**) and OCT-based measurements of diameters of a lamellar macular hole with standard ERM and LHEP, taken at the level of the ILM (**C**), OPL (**D**), and Schis/Cav (**E**). The *vertical white arrow* on B-FAF image in **B** indicates the location of the corresponding OCT scans; the caliper indicates where the vertical diameter of the hole was measured on B-FAF image.

increase ($P < 0.001$), and the presence of LHEP led to a nonsignificant increase in B-FAF diameter.

Conversely, the relationship between B-FAF and OPL diameter differed for the eyes with ERM alone and those with LHEP. Specifically, B-FAF diameter increased by 89 µm per 100-µm increase in OPL diameter in the ERM alone group and by 75 µm per 100-µm increase of OPL diameter in the LHEP group ($P < 0.001$).

Because of evident heteroschedasticity for schisis/cavitation (observed in the reference B-FAF/OCT scan in only 66 eyes) and sparse data for EZ disruption (observed in the reference scan in only 3 eyes with standard ERM and in 23 eyes with LHEP) Spearman's ρ instead of Pearson's correlation coefficient was used to examine the correlation of these two variables with B-FAF diameter. No relationship was found between B-FAF diameter and schisis/cavitation diameter (larger than the B-FAF diameter in every case, $r = 0.05$) or EZ disruption length ($r = 0.0$).

Interrater Agreement

The ICC between observers for the grading of B-FAF diameter was 0.98 (95% CI: 0.96 to 0.99) and 0.98 (95% CI: 0.97 to 0.99) for LMHs with standard ERM and LHEP, respectively, and the ICC for the grading of OPL diameter was 0.98 (95% CI: 0.97 to 0.99) for both LMHs with standard ERM and LHEP. Similar results were found for the diameters measured at ILM and schisis/cavitation levels (0.98 in both cases) and the EZ disruption length (0.97). The κ coefficient for the attribution of the presence of EZ disruption lines was 0.94.

Discussion

In this study, we show that, in eyes with LMHs, independently from the associated epiretinal material, a strong correlation exists between the diameters of the holes measured from B-FAF images and those measured at the OPL level from OCT images.

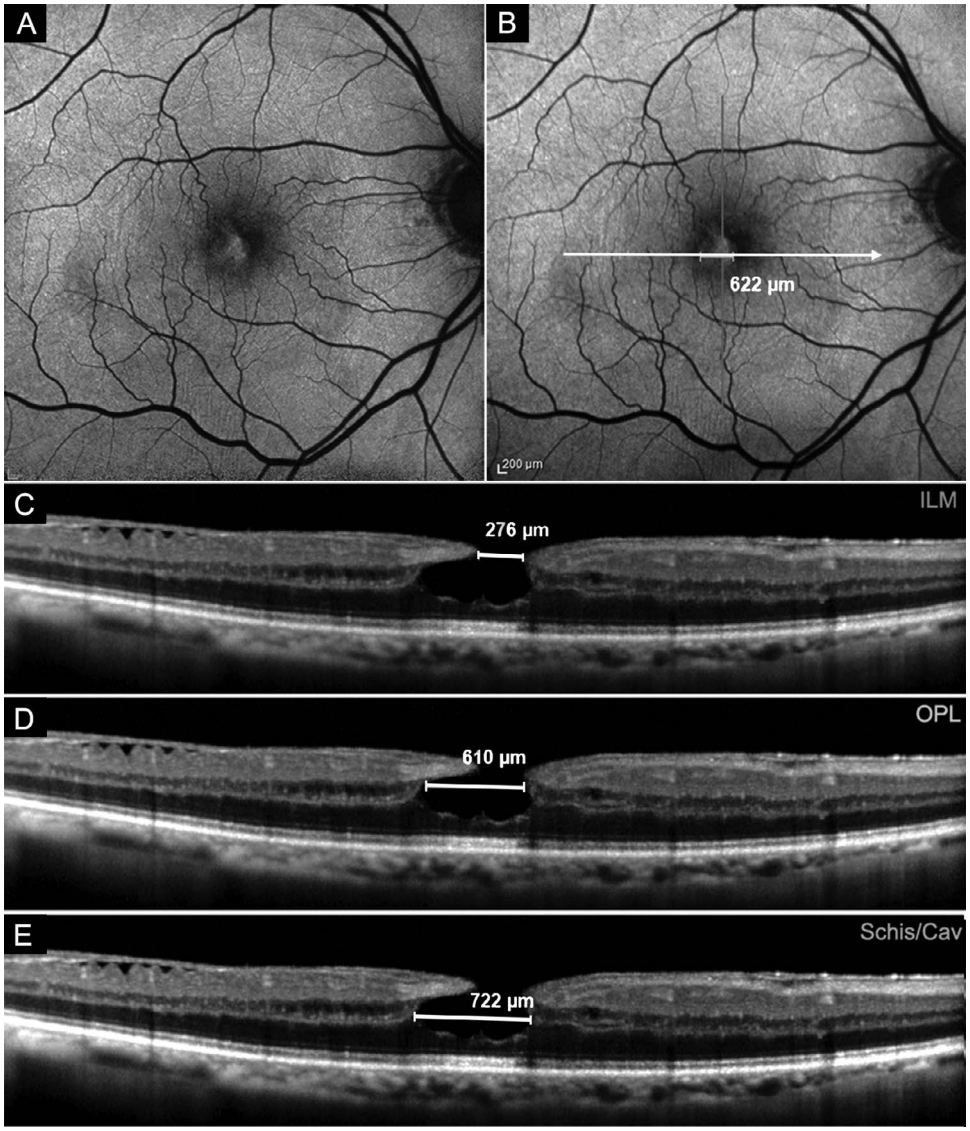

FIGURE 4. B-FAF (**A**, **B**) and OCT-based measurements of diameters of a lamellar macular hole with LHEP, taken at the level of the ILM (**C**), OPL (**D**), and Schis/Cav (**E**). The *horizontal white arrow* on the B-FAF image indicates the location of the corresponding OCT scans; the caliper indicates where the horizontal diameter of the hole was measured on B-FAF image.

Thus, we suspect that loss or displacement of retinal tissue within the OPL layer might be the main culprit of the increased B-FAF signal observed in eyes affected by LMHs associated with either standard ERM alone or LHEP.

SD-OCT technology has provided dramatically improved resolution of the retinal architecture that allows for more detailed analyses of the morphology and progression of vitreomaculopathies including LMHs. On the basis of SDOCT features[7–10] and histopathology studies,[13–15] two main types of LMHs have been established; they are distinguished mainly by the associated epiretinal material, which can appear as either thin and highly reflective (standard ERM) or thick with medium reflectivity (the so-called LHEP) in OCT imaging.

Despite these defining features, both types of LMHs share similar characteristics on B-FAF, in the form of increased autofluorescence signals corresponding to the hole area. This increased signal might be caused by (1) presence of subretinal autofluorescent deposits or foveal detachment; (2) loss/rarefaction of photoreceptors; (3) loss of retinal tissue containing MP; and (4) centrifugal displacement of the retinal tissue containing MP. Because the first were exclusion criteria in the current study, they will not be included in further discussions herein, whereas the other hypotheses deserve further examination.

In regard to the loss/rarefaction of photoreceptors, unbleached photoreceptor pigment has a similar, although lesser, effect on the appearance of B-FAF as MP, as it absorbs and therefore attenuates the excitation light available to elicit autofluorescence at the level of the RPE.[16,17] Consequently, areas with photoreceptor loss (and reduced photoreceptor pigment density) show increased B-FAF levels relative to surrounding areas with healthy photoreceptors. In the literature, the integrity of the outer retinal bands (ORBs) and especially of the EZ is generally used as a surrogate for assessing the health of the photoreceptors at the fovea. According to previous reports, disruption of EZ is much more common in LMHs with LHEP than in LMHs with ERM alone, but all LMHs show an increased autofluorescence signal, independent of the integrity/disruption of EZ. In this study, no correlation was found between the length of disrupted EZ and

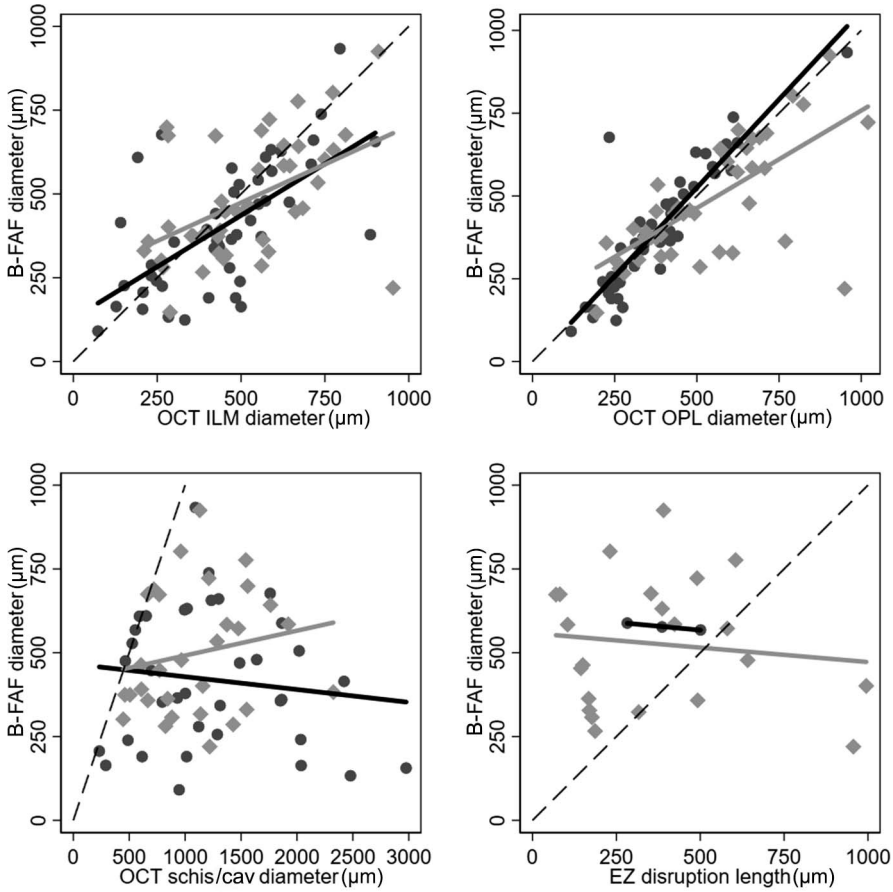

FIGURE 5. Correlations between B-FAF and OCT-based measurements of diameters of lamellar macular hole taken at the level of the ILM, OPL, Schis/Cav, and length of disrupted EZ in eyes with standard ERM alone (*black dots* and *solid black line*) and LHEP (*gray diamonds* and *solid gray line*) respectively. The *solid lines* represent the linear fit obtained with univariate regression model in each group, whereas the *dashed line* is the equivalence line.

B-FAF diameter in the LHEP group, which was the only one in which this correlation could be explored because EZ disruption was only present in 6.4% of the eyes with ERM alone. Thus, although photoreceptor defects may contribute to the increased autofluorescence signal, it is unlikely that these defects are the main cause of the increased signal observed in eyes with LMHs.

To test the validity of the other two hypotheses (loss or centrifugal displacement of the retinal tissue containing MP), we explored the correlation between diameters measured with B-FAF and OCT imaging at three different levels (ILM, OPL, and schisis/cavitation).

In fact, although by definition, OCT-based features of LMH include an irregular foveal contour and a defect in the inner fovea, it is unknown which lost/displaced retinal layer causes the increased autofluorescence signal.

Specifically, we decided to take measurements of the distance between the central borders of the OPL for two reasons: (1) the splitting or cavitation of the retina in eyes with LMHs typically occurs between the outer plexiform and outer nuclear layer; and (2) the outer two-thirds of the OPL at the fovea are constituted by the Henle fiber layer that is the foveal site where the MP is mainly localized.[18]

As reported above, we found a strong correlation between B-FAF diameter and diameters measured at the OPL levels on OCT in both the ERM-alone group and the LHEP group. The slightly different correlation found in the cases with and without LHEP (B-FAF diameter increased by 89 µm per 100-µm increase in OPL diameter in the ERM alone group and by 75 µm per 100-µm increase of OPL diameter in the LHEP group) is likely related to the shape and morphology of the hole in the two groups. Specifically, the presence of a cavitation and LHEP may have made precise identification of OPL borders more difficult to achieve in some of the cases. In particular, the pigment present in LHEP tissue, may have partly obscured the underlying autofluorescent signal, causing an underestimation of its diameters. Conversely, a moderate correlation was found between B-FAF and ILM diameters. Such observations suggest that the increased autofluorescent signal seen in eyes with LMH is mainly related to a missing OPL tissue rather than to the lack of innermost retinal layers. This is in line with the observation that the intensity of the increased autofluorescence signal does not correlate with the thickness of the residual retinal tissue (comprised of the outer part of ONL) in eyes with LMHs.[9]

Whether this missing OPL tissue is truly lost or merely dislocated remains an issue unresolved by the current imaging capabilities. Nevertheless, in light of the results of this study and the data from the literature, some considerations can be made. Histopathologic studies suggest tractional forces are primarily responsible for LMHs associated with standard ERM,[13–15] whereas LMHs with LHEP would be the consequence of a slow, chronic, degenerative process.[8] Lamellar macular holes with ERM alone generally show better BCVA and integrity of the ORBs, whereas a worse BCVA, a severely reduced foveal thickness, and abnormalities at the level of the

ORBs are usually observed in eyes with LMHs associated with LHEP. Outcomes after surgery, at least in terms of final BCVA reached and restoration of foveal contour, are superior in eyes with standard ERM alone than in eyes with LHEP.[10,13–15] Finally, in the current study, we found that the diameters of increased B-FAF are significantly greater in eyes with LHEP than in eyes with standard ERM alone.

Taken together, these data indicate that a true loss of tissue, if occurring, is more likely in LMHs with LHEP than in LMHs with standard ERM alone. Nevertheless, future studies that calculate the total amount of MP are warranted to better address this issue. In fact, as observed in eyes with other macular pathologies affecting MP like type 2 macular telangiectasia, lutein and zeaxanthin could not be lost from the posterior fundus, but rather displaced laterally to a certain extent.[19] Similarly, in eyes with LMH, the retinal tissue containing the pigment could be dislodged from its original location; specifically, in eyes with standard ERM, the MP could be displaced centrifugally, whereas in the eyes with LHEP, some pigment could have migrated in this peculiar epiretinal tissue. In fact, the presence of carotenoid in surgically removed LHEP has been recently reported in eyes operated on for LMH.[20]

In any case, the lack of MP at the fovea, either from displacement or loss of tissue, represents the absence of a foveal constituent that would be there under typical circumstances. Given the difficulties in defining a lamellar defect in the fovea on SDOCT-based imaging, the B-FAF features of LMH should be thoroughly evaluated toward informing future, more precise definitions.

It is likely that both photoreceptors and Müller cells, the only cells constituting the central part of the fovea, play a crucial role for the displacement/loss of MP and the formation of LMH. Specifically, the involvement of Müller cells is suggested by the following aspects: (1) they provide the structural stability of the fovea[21] and foveal contour is irregular by definition in LMH; (2) they contain MP at high density at the fovea[22] and an increased autofluorescence signal (due to lack of MP) is typically seen in association with LMH; and 3) there is histologic evidence of proliferating Müller cells within the LHEP tissue.[23]

This study has some limitations, mainly based on the relatively small sample size and on the manual measurements of B-FAF and OCT diameters. However, current built-in software does not yet allow automatic calculation of the distances between hole borders; furthermore, the values of weighted κ statistics and ICCs showed excellent repeatability and consistency of data collected separately by two graders. The strengths of this study include the use of an OCT device that is able to simultaneously record B-FAF and OCT images and the correlations investigated between B-FAF and OCT diameters measured at three different levels.

In conclusion, we show that a strong correlation exists between diameters of the hole measured with B-FAF and diameters of the hole measured at the OPL level on OCT imaging in eyes with LMHs. This may imply that the loss or displacement of retinal constituents containing MP located at the OPL level, specifically photoreceptor axons and/or Müller cells, are mainly involved in this vitreomaculopathy.

Acknowledgments

Disclosure: **R. dell'Omo**, None; **D. Vogt**, None; **R.G. Schumann**, None; **S. De Turris**, None; **G. Virgili,** None; **G. Staurenghi**, Heidelberg Engineering (C), Quantel Medical (C), Zeiss (C), Alcon (C), Allergan (C), Bayer (C), Boheringer (C), Genentech (C), GSK (C), Novartis (C), Roche (C), Ocular Instruments (R), Optos (F), Centervue (F); **M. Cereda**, Bayer (C); **C. Costagliola**, None; **S.G. Priglinger**, None; **F. Bottoni**, Bayer (S), Novartis (S), Alcon (R)

References

1. Delori FC, Dorey CK, Staurenghi G, Arend O, Goger DG, Weiter JJ. In vivo fluorescence of the ocular fundus exhibits retinal pigment epithelium lipofuscin characteristics. *Invest Ophthalmol Vis Sci*. 1995;36:718–729.
2. von Rükmann A, Fitzke FW, Bird AC. Distribution of fundus autofluorescence with a scanning laser ophthalmoscope. *Br J Ophthalmol*. 1995;79:407–412.
3. Schmitz-Valckenberg S, Holz FG, Bird AC, Spaide RF. Fundus autofluorescence imaging: review and perspectives. *Retina*. 2008;28:385–409.
4. Snodderly DM, Auran JD, Delori FC. The macular pigment. II. Spatial distribution in primate retinas. *Invest Ophthalmol Vis Sci*. 1984;25:674–685.
5. von Rükmann A, Fitzke FW, Bird AC. Distribution of pigment epithelium autofluorescence in retinal disease state recorded in vivo and its change over time. *Graefes Arch Clin Exp Ophthalmol*. 1999;237:1–9.
6. von Rükmann A, Fitzke FW, Gregor ZJ. Fundus autofluorescence in patients with macular holes imaged with a laser scanning ophthalmoscope. *Br J Ophthalmol*. 1998;82:346–351.
7. Pang CE, Spaide RF, Freund BK. Comparing functional and morphologic characteristics of lamellar macular holes with and without lamellar hole-associated epiretinal proliferation. *Retina*. 2015;35:720–726.
8. Govetto A, Dacquay Y, Farajzadeh M, et al. Lamellar macular hole: two distinct clinical entities? *Am J Ophthalmol*. 2016;164:99–109.
9. Bottoni F, Carmassi L, Cigada M, Moschini S, Bergamini F. Diagnosis of macular pseudoholes and lamellar macular holes: is optical coherence tomography the "gold standard"? *Br J Ophthalmol*. 2008;92:635–639.
10. dell'Omo R, Virgili G, Rizzo S, et al. Role of lamellar hole-associated epiretinal proliferation in lamellar macular holes. *Am J Ophthalmol*. 2017;175:16–29.
11. Duker JS, Kaiser PK, Binder S, et al. The international vitreomacular traction study group classification of vitreomacular adhesion, traction, and macular hole. *Ophthalmology*. 2013;120:2611–2619.
12. Bottoni F, Zanzottera E, Carini E, Cereda M, Cigada M, Staurenghi G. Re-accumulation of macular pigment after successful macular hole surgery. *Br J Ophthalmol*. 2016;100:693–698.
13. Parolini B, Schumann RG, Cereda MG, Haritoglou C, Pertile G. Lamellar macular hole: a clinicopathologic correlation of surgically excised epiretinal membranes. *Invest Ophthalmol Vis Sci*. 2011;52:9074–9083.
14. Schumann RG, Compera D, Schaumberger MM, et al. Epiretinal membrane characteristics correlate with photoreceptor layer defects in lamellar macular holes and macular pseudoholes. *Retina*. 2015;35:727–735.
15. Compera D, Entchev E, Haritoglou C, et al. Lamellar hole-associated epiretinal proliferation in comparison to epiretinal membranes of macular pseudoholes. *Am J Ophthalmol*. 2015;160:373–384.
16. Theelen T, Berendschot TT, Boon CJ, Hoyng CB, Klevering BJ. Analysis of visual pigment by fundus autofluorescence. *Exp Eye Res*. 2008;86:296–304.
17. Sommerburg O, Siems WG, Hurst JS, Lewis JW, Kliger DS, van Kuijk FJ. Lutein and Zeaxanthin are associated with photoreceptors in the human retina. *Curr Eye Res*. 1999;19:491–495.

Investigative Ophthalmology & Visual Science

18. Bone RA, Landrum JT, Friedes LM, et al. Distribution of lutein and zeaxanthin stereoisomers in the human retina. *Exp Eye Res*. 1997;64:211–218.
19. Degli Esposti S, Egan C, Bunce C, Moreland JD, Bird A, Robson AG. Macular pigment parameters in patients with macular telangiectasia (MacTel) and normal subjects; implications of a novel analysis. *Invest Ophthalmol Vis Sci*. 2012;53:6568–6575.
20. Obana A, Sasano H, Okazaki S, Otsuki Y, Seto T, Gohto Y. Evidence of carotenoid in surgically removed lamellar hole-associated epiretinal proliferation. *Invest Ophthalmol Vis Sci*. 2017;58:5157–5163.
21. Gass JD. Müller cell cone, an overlooked part of the anatomy of the fovea centralis. *Arch Ophthalmol*. 1999;117:821–823.
22. Syrbe S, Kuhrtb H, Gärtnerc U, et al. Müller glial cells of the primate foveola: an electron microscopical study. *Exp Eye Res*. 2018;167:110–117.
23. Pang CE, Maberley DA, Freund KB, et al. Lamellar hole-associated epiretinal proliferation. A clinicopathologic correlation. *Retina*. 2016;36:1408–1412.

Investigative Ophthalmology & Visual Science